Journal of Power Sources 196 (2011) 2709–2716

Contents lists available at ScienceDirect

Journal of Power Sources

journal homepage: www.elsevier.com/locate/jpowsour

Compliant alkali silicate sealing glass for solid oxide fuel cell applications: Thermal cycle stability and chemical compatibility

Yeong-Shyung Chou[a,*], E.C. Thomsen[a], R.T. Williams[a], J.-P. Choi[a], N.L. Canfield[a], J.F. Bonnett[a], J.W. Stevenson[a], A. Shyam[b], E. Lara-Curzio[b]

[a] K2-44, Energy and Efficiency Division, Pacific Northwest National Laboratory, P.O. Box 999, Richland, WA 99354, United States
[b] Materials Science and Technology Division, Oak Ridge National Laboratory, P.O. Box 2008, Oak Ridge, TN 37831, United States

ARTICLE INFO

Article history:
Received 23 September 2010
Received in revised form 3 November 2010
Accepted 4 November 2010
Available online 11 November 2010

Keywords:
Sealing glass
Leak rate
Coating
SOFC

ABSTRACT

An alkali silicate glass (SCN-1) is currently being evaluated as a candidate sealing glass for solid oxide fuel cell (SOFC) applications. The glass containing ~17 mole% alkalis (K_2O and Na_2O) remains vitreous and compliant during SOFC operation, unlike conventional SOFC sealing glasses, which experience substantial devitrification after the sealing process. The non-crystallizing compliant sealing glass has lower glass transition and softening temperatures since the microstructure remains glassy without significant crystallite formation, and hence can relieve or reduce residual stresses and also has the potential for crack healing. Sealing approaches based on compliant glass will also need to satisfy all the mechanical, thermal, chemical, physical, and electrical requirements for SOFC applications, not only in bulk properties but also at sealing interfaces. In this first of a series of papers we will report the thermal cycle stability of the glass when sealed between two SOFC components, i.e., a NiO/YSZ anode supported YSZ bilayer and a coated ferritic stainless steel interconnect material. High temperature leak rates were monitored versus thermal cycles between 700 and 850 °C using back pressures ranging from 1.4 to 6.8 kPa (0.2–1.0 psi). Isothermal stability was also evaluated in a dual environment consisting of flowing dilute H_2 fuel versus ambient air. In addition, chemical compatibility at the alumina and YSZ interfaces was examined with scanning electron microscopy and energy dispersive spectroscopy. The results shed new light on the topic of SOFC glass seal development.

1. Introduction

Solid oxide fuel cells are an emerging technology which not only can reach very high energy conversion efficiency (over 60%) but also offer great opportunities for carbon capture, due to separate fuel and air flow streams [1,2]. In SOFCs, electrical energy is extracted from the electrochemical reaction of fuels like hydrogen or carbon monoxide with oxidants like air. Oxygen is ionized at the cathode/electrolyte interface and transported through vacancies in the electrolyte to the anode, where the oxygen reacts with hydrogen to form water and releases electrical energy as well as thermal energy. To increase the power density, many SOFC developers are pursuing planar designs in which repeating unit cells are stacked and connected electrically in series. Planar stack designs typically require several different seals, such as ceramic cell to window frame seals, seals between interconnect plates, and seals between end plates which provide gas inlets and outlets. Sealing of planar stacks represents one of the primary challenges facing SOFC developers, so development of a reliable sealant or sealing system remains one of the top priorities in advancing planar SOFC technology. For glass seals, the challenges lie not only in satisfying the initial requirements such as hermeticity or allowable leak rates through optimization of the bulk glass properties, but also in controlling reactivity at the sealing interfaces. The very harsh SOFC operating conditions, i.e., elevated temperatures and dual environments, and requirement of a lifetime up to 40,000 h with hundreds to thousands of thermal cycles make glass seal development a most challenging hurdle [3].

To date, SOFC glass seal research has been focused mainly on glass–ceramic approaches in which the initial glass devitrifies into a rigid or semi-rigid glass–ceramic mixture after the sealing processes [4–12]. Previously, alkaline earth-based aluminosilicate glasses have been extensively studied as candidate sealing glasses [5–19]. Lahl et al. studied the crystallization kinetics of $AO–Al_2O_3–SiO_2–B_2O_3$ glasses (A = Ba, Ca, Mg) and the influence of nucleating agents [9]. Sohn et al. investigated the thermal and chemical stability of the $BaO–Al_2O_3–La_2O_3–SiO_2–B_2O_3$ system [10]. Ley et al. studied the system of $SrO–Al_2O_3–La_2O_3–SiO_2–B_2O_3$ and thermal expansion behaviors [6]. Other systems of phosphate glasses [11], borosilicate glasses [4], and ceramic fiber reinforced

* Corresponding author. Tel.: +1 509 3752527; fax: +1 509 3752186.
E-mail address: yeong-shyung.chou@pnl.gov (Y.-S. Chou).

0378-7753/$ – see front matter © 2010 Published by Elsevier B.V.
doi:10.1016/j.jpowsour.2010.11.020

glass [5] have also been investigated. However, the CTEs of these glasses were in the low range, e.g., ~5.7–7.9 × 10^{-6} °C^{-1} for the phosphate glasses, which resulted in poor thermal cycle stability [11]. A good example of a state-of-the-art sealing glass is a Ba–Ca–Al–B silicate glass–ceramic developed by Pacific Northwest National Laboratory [12]. This glass has a very good CTE match with the SOFC components after initial crystallization (CTE ~ 12.5 × 10^{-6} °C^{-1} 750 °C/4 h). The CTE, however, decreases to ~11 × 10^{-6} °C^{-1} after ageing at 750 °C for 1000 h, which could cause problems during repeated thermal cycling. To retain constant CTE over ageing and minimize use of Ba, a Sr–Ca–Y–B silicate glass system was developed that shows very promising thermal and electrical stability [13–16].

As mentioned above the glass–ceramic sealants develop a rigid or semi-rigid microstructure after substantial crystallization, resulting from the fact that a "glass" is in a meta-stable state and thermodynamically will prefer to rearrange its random structure to lower the free energy. The typical SOFC operating condition of ~700–900 °C provides substantial thermal energy for atoms to reorganize themselves into a crystalline structure. As a result, the matching of CTEs is very critical for the glass–ceramic type of sealants. To avoid this constraint, a novel approach using a glass resistant to crystallization was sought such that, after heat treatment, the sealing glass will remain vitreous and retain the softening or compliant behavior to relieve stresses [17]. In addition, should cracks form during cooling to room temperature they may heal upon re-heating of the stack for routine operation. Crack healing has been observed in glasses at elevated temperatures [17,18]. However, the ability to maintain a vitreous state without crystallization at SOFC operation conditions over the long term remains unknown. Most of the glass–ceramic candidates contain no alkalis and the effect of alkalis appears unclear. In this paper, we will present the first part of a series of studies on a commercially available alkali silicate glass, with an emphasis on thermal property characterization and leak behavior at various temperatures and back pressures. High temperature leak rates will be reported for cycling and ageing tests. Of particular interest is the chemical compatibility with SOFC components such as YSZ electrolyte and metallic interconnect. Results of post-mortem microstructure and interfacial analysis will be discussed to assess the suitability of the compliant glass approach for SOFC applications. The second part of the work, involving volatility, electrical, and mechanical properties, will be reported in the future.

2. Experimental

2.1. Chemical composition and thermal properties characterization

The glass under study is a commercial alkali silicate glass (SCN-1, SEM-COM, Toledo, OH). The chemical composition, as determined by inductively coupled plasma-optical emission spectroscopy (ICP-OES), is listed in Table 1. The silicate glass contains alkaline earths, mainly BaO (8.23 mole%) and CaO (3.34 mole%), alkalis of K_2O (10.0 mole%) and Na_2O (7.3 mole%), Al_2O_3 (2.8 mole%), and some impurities (less than 1%) of Fe, Mg and Ti. Thermal properties of glass transition (T_g), softening point (T_s), and average coefficient of linear thermal expansion (CTE) were determined by thermal mechanical analysis using sintered glass bars of 3 mm × 3 mm × 5 mm.

2.2. Sample preparation and coupon sealing

To mimic actual SOFC conditions, the candidate sealing glass was sealed between a NiO/YSZ anode-supported thin YSZ electrolyte bi-layer and a ferritic stainless steel (SS441) square substrate. The ceramic bi-layer was fabricated by a conventional tape casting and lamination process, punched into discs, and sintered at ~1400 °C in air. The as-sintered discs were creep flattened at a lower temperature (~1350 °C) under a dead weight equivalent to ~7 kPa. The discs were circular in shape with 35.6 mm diameter and a total thickness of 550 μm including a thin and dense YSZ electrolyte layer of ~10 μm after sintering. The metal substrate was a square of 50 mm × 50 mm × 1 mm with a central hole of 6.35 mm diameter machined from larger SS441 sheets (ATI Allegheny Ludlum, Pittsburgh, PA). Stainless steel SS441 is currently considered a candidate metallic interconnect for planar SOFC applications, due to matching CTEs with NiO–YSZ anode (both SS441 and NiO–YSZ anode have average CTEs in the range of 12–13 × 10^{-6} °C^{-1} from room temperature to elevated temperatures), ability to form a conductive oxide layer, and reasonable low cost. However, the metal contains an appreciable amount of Cr, which can cause poisoning of cathodes as well as mechanical degradation in sealing areas by forming chromates with very high CTEs if sealing glasses containing alkaline earths (e.g., Ba and Sr) are used [13,14,19]. As a result, a protective coating is required for the sealing area, in addition to the active cathode area. In this study we have adopted a novel reactive air aluminizing coating process involving ultrasonic spraying of SS441 substrates with a mixture of Al powders in a binder solution, followed by drying and oxidizing at 1000 °C for 1 h in air [20]. To contain the low viscosity sealing glass, two concentric rings of 8YSZ ceramic (~225 μm thick) with different diameters were also fabricated using the same tape casting and heat treatment process as the ceramic bilayers. Fig. 1 shows the preparation of the test couples with glass paste on the bilayer disc between two concentric YSZ rings, and the sintered couple, in A and B, respectively. The sintering was conducted at 800 °C for 2 h in air with a small dead weight to ensure good contact.

Table 1
Chemical composition of SCN-1 glass (wt%) determined by ICP-OES.

Oxide	wt%
$A1_2O_3$	2.81
BaO	8.23
CaO	3.34
Fe_2O_3	0.22
K_2O	10
MgO	0.62
Na_2O	7.29
TiO_2	0.54
ZnO	0.01
ZrO_2	0.01
Li_2O	0.02
B_2O_3	0.03
SiO_2	66.86

2.3. Leak test, thermal cycling, ageing in dual environment, and characterization

The as-sealed couples (Fig. 1B) were first leak checked at room temperature using iso-propanol, by applying the alcohol in the central cavity and observing if any alcohol penetrated through the glass seal to the other side. Only hermetic samples, i.e., no alcohol penetration, were used for thermal cycle and ageing stability tests. The sample was then pressed at 82–163 kPa between a leak tester made of Inconel600 and an alumina support for thermal cycle and ageing stability tests, as shown in Fig. 2. A hybrid mica seal with Ag or SCN-1 glass as the interlayer was used for the perimeter seal [3]. Thermal cycling was conducted in ambient air from room temperature to elevated temperatures of 700, 750, 800, and 850 °C. It took 3 h to heat to the elevated temperatures; the furnace was then held for 3 h while measuring the leak rates, and then cooled to room temperature in 18 h so that a full thermal cycle took 24 h. Leakage

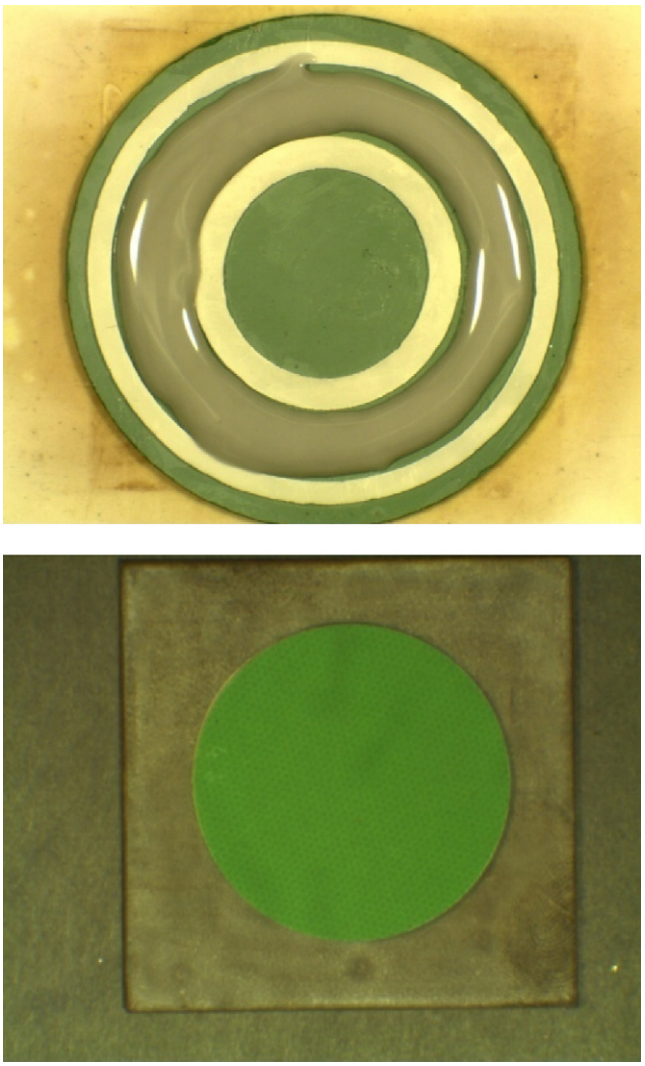

Fig. 1. Optical micrograph shows the sample preparations for coupon sealing. (A) Glass paste (gray) applied between two concentric YSZ rings (white) on the ceramic bi-layer disc (green), and (B) the ceramic bilayers disc sealed onto an aluminized SS441 square substrate. (For interpretation of the references to color in this figure legend, the reader is referred to the web version of the article.)

was measured with ultra-high purity helium at a differential pressure of ~1.4–6.8 kPa (0.2–1 psi), and represented as standard cubic centimeters per minute per leak length (sccm cm^{-1}) [3]. In addition to thermal cycling tests, ageing tests in a dual environment were also conducted at 750 and 800 °C for ~1000 h with flowing 5% H_2/N_2 (with ~3% H_2O) inside the test chamber surrounded by ambient air. During the ageing test a back pressure of 6.8 kPa (1 psi) was established by flowing the gas through a column of water. After the ageing test, the sample was checked with optical microscopy, followed by cutting and polishing for microstructure and chemical analysis with scanning electron microscopy (SEM) and energy dispersion spectroscopy (EDS) (JOEL SEM model 5900LV).

3. Results and discussion

3.1. Thermal expansion behavior of non-crystallizing SCN-1 glass and conventional crystallizing sealing glass

Fig. 3A shows the thermal expansion behavior of SCN-1 glass during three heating and cooling cycles. For comparison, a conventional glass–ceramic type of refractory sealing glass is also included (Fig. 3B). It is evident the SCN-1 glass has much different thermal expansion behaviors as compared to the crystallizing glass–ceramics. For example, the SCN-1 glass still shows the typical glass expansion behavior with distinct glass transition point and softening points. The glass transition temperature increased slightly from 468 °C (1st cycle at 0.1 N) to 486 °C (2nd cycle at 0.05 N), and 494 °C (3rd cycle at 0.01 N) while the softening point increased from 540 °C (1st cycle) to 585 °C (2nd cycle), and ~600 °C (3rd cycle). After ageing for 500 h in air at 800 °C the linear expansion curve (not shown here) was very similar to the as-sintered one, with a slightly higher glass transition point of 509 °C. On the other hand, a conventional glass–ceramic sealant (YSO1) showed a significant change in thermal expansion behavior after short-term heat treatment at 1000 °C/1 h and 800 °C/4 h. After the heat treatment, the material showed linear expansion behavior up to the softening point, suggesting drastic microstructure and phase changes. The glass transition point of the as-prepared YSO1 glass was 695 °C and softening point was 733 °C while the heat-treated (crystallized) material showed no obvious transition point and much higher softening at 880 °C [13].

3.2. Design of leak test fixture

Fig. 2 shows a leak test fixture which was designed for evaluating high temperature seals. For SOFC applications, the normal operation temperature ranges from ~700 °C to ~850 °C for planar designs and could be close to ~950 °C for tubular or electrolyte-supported cells. To measure the high temperature leak rates during repeated thermal cycling is not trivial, as the test fixture needs to have high temperature strength, very good oxidation resistance, stability in humid reducing environment, matching CTEs, and availability in block and tube forms. Unfortunately no single material meets all the requirements to the best knowledge of the authors. Inconel600 and alumina were chosen as the primary fixture materials, with hybrid mica seals around the perimeter. The total leak rate measured during the leakage tests was the sum of the leak rate through the hybrid mica perimeter seal plus the leak rate through the glass seal. Given a known leak rate through the hybrid mica perimeter seal, one can then subtract that value to obtain the leakage (if any) through the glass seal. The choice of this indirect method appears to be unavoidable given that no glass seal can tolerate the large CTE mismatch between the Inconel600 top fixture (~16–17 × 10^{-6} °C^{-1}) and SS441. Welding the Inconel600 fixture with SS441 substrate would induce severe thermal stresses which can easily damage the glass seal to be tested since the ceramic bilayer would already be sealed onto the metal substrate, not to mention issues involving welding of dissimilar materials. One could braze the metal substrate to the Inconel600 top fixture, however, the large residual stresses from CTE mismatches between Inconel600, braze, and aluminized SS441 would still create uncertainty regarding the braze stability during thermal cycling. Should the braze start to leak with an unknown and changing leak rate during the test, one could not accurately determine the leak rate of the glass seal under test. Also, post mortem de-assembly could very well fracture the glass seal. As a result, hybrid mica was chosen as the perimeter seal for the test fixture. The hybrid mica seal has been shown to have fairly constant leak rates during thermal cycle testing up to 1000 cycles and long-term ageing stability up to ~28,400 h at 800 °C [21,22]. In addition, de-assembly of the test fixture after testing is unlikely to damage the glass seal, since the compressive mica seal does not bond strongly with mating surfaces, allowing for post-mortem leak checking with isopropanol.

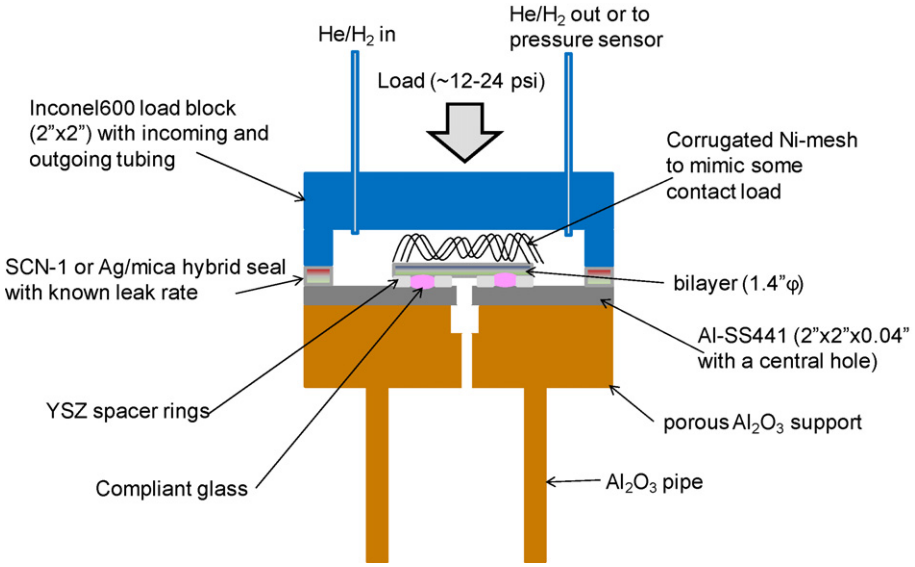

Fig. 2. Schematic drawing shows the assembly of leak test fixture for glass sealed between a ceramic bi-layer and an aluminized SS441 substrate. The sample was pressed between an Inconel600 top fixture and an alumina bottom support with hybrid mica as the perimeter seal. The glass was contained between two concentric rings spacer made of YSZ ceramics.

3.3. Effect of temperature on thermal cycle stability at various back pressures

Results of thermal cycle stability tests of SCN-1 glass at various temperatures and different helium pressures for cycling from room temperature to 850 °C, 800 °C, 750 °C, and 700 °C are shown in Fig. 4A–D, respectively. For thermal cycling to 800 °C (Fig. 4B) only leak rates tested at 1.4 kPa (0.2 psi) are reported. Leak rates at the other three temperatures were also measured at higher helium pressures. The measured leak rates, as mentioned in previous section, are the summation of all leak paths, through the glass seal and the mica seal. It is evident that the leak rates at low helium pressure of 1.4 kPa are all within 0.01–0.05 sccm cm^{-1}, consistent with typical hybrid mica seals at similar compressive stresses [3,21,22]. It is noted that the mica paper used for this study is ~200–300 μm thick and is composed of discrete mica flakes of varying sizes (hundreds to thousands of microns in size and thickness less than 10 μm) overlapping with each other. As a result, the pore microstructure of each mica sheet will be different and lead to a range of leak rate measurements. However, leaks in the observed range are much less than would be expected with a typical glass seal failure. It was found from our earlier study that brittle fracture of a rigid glass seal of similar geometry would result in substantially higher leak rates, as much as 8 times higher. For example, the hybrid phlogopite mica with glass–ceramic (G18, Ba–Ca–Al–B-silicate [12]) interlayers turned into a rigid monolithic ceramic after isothermal ageing at 800 °C for ~1000 h, due to reaction of G18 glass with mica (aluminosilicate in layer structure). As a result, the 800 °C leak rates after some thermal cycles increased substantially from ~0.04 sccm cm^{-1} to ~0.32 sccm cm^{-1} [22]. Therefore, the leak rates measured in the present study clearly suggested that the SCN-1 glass had very good thermal cycle stability without fracture during cooling (or, if fracture occurred, it may have healed upon re-heating). The fairly constant leak rates at all temperatures are consistent with the thermal cycle stability of hybrid micas. The leak rates at various helium pressures (~3.4–6.8 kPa) appeared to be linearly proportional to the pressure, as previously observed in hybrid mica seals. For example, the average 750 °C leak rates (Fig. 4C) are 2.9×10^{-2} sccm cm^{-1} ($\pm 0.5 \times 10^{-2}$), 8.0×10^{-2} sccm cm^{-1} ($\pm 0.8 \times 10^{-2}$), and 16.1×10^{-2} sccm cm^{-1} ($\pm 1.4 \times 10^{-2}$), proportional to the helium pressure at 1.4 kPa (0.2 psi), 3.4 kPa (0.5 psi), and 6.8 kPa (1.0 psi), respectively.

3.4. Isothermal ageing in dual environments

In addition to pure thermal cycling tests, isothermal ageing stability testing was also conducted with dual environments of flowing dilute hydrogen (with ~3% H_2O) inside the test fixture surrounded by ambient air at 750 and 800 °C. Upon completion of 1000 h ageing the sample was further subjected to a few thermal cycles to room temperature. The leak rates during isothermal ageing are shown in Fig. 5A and B for 750 and 800 °C, respectively. It is evident the seal based on SCN-1 glass was hermetic with a majority of leak rates less than ~0.01 sccm cm^{-1}, and no dependence on helium pressure. For these two samples SCN-1 glass was also used as the compliant interlayers of the hybrid mica perimeter seal (see Fig. 3), instead of thin (25 μm thick) Ag foil. The SCN-1 glass on the mica was much thicker (a few hundreds of microns) and was under compressive stresses. As a result of the 800 °C sealing process, some of the low viscosity glass was squeezed out. The extra glass apparently coalesced and sealed off the edges of the perimeter mica, resulting in observed the hermetic behavior (i.e., independent of helium pressure). Most importantly, however, the SCN-1 glass did demonstrate the desired thermal stability in dual environments. These two samples were then subjected to a few thermal cycles to room temperature. Leak rates of the 800 °C sample after 4 thermal cycles showed a substantial increase to ~0.19 sccm cm^{-1}, ~0.42 sccm cm^{-1}, and ~0.58 sccm cm^{-1} for the helium pressure at 1.4 kPa, 3.4 kPa, and 6.8 kPa, respectively. Similar drastic increase of leak rates was also observed for the 750 °C sample, where the leak rates were ~0.38 sccm cm^{-1}, ~0.69 sccm cm^{-1}, and ~1.1 sccm cm^{-1} at these three pressures. Clearly, these leak rates were much larger than those of typical hybrid micas, indicating fracture of glass seal or ceramic bilayers. Upon post-mortem analysis, it was found that the ceramic bilayer disc fractured in both cases. In the previous pure thermal cycling tests, no bilayer fracture was observed with the same materials set and geometry. Clearly the cause of bilayers fracture could not be solely attributed to the residual stresses from CTE mismatch between the thick YSZ spacer rings (CTE ~ 10.5×10^{-6} °C^{-1}) and mating SOFC

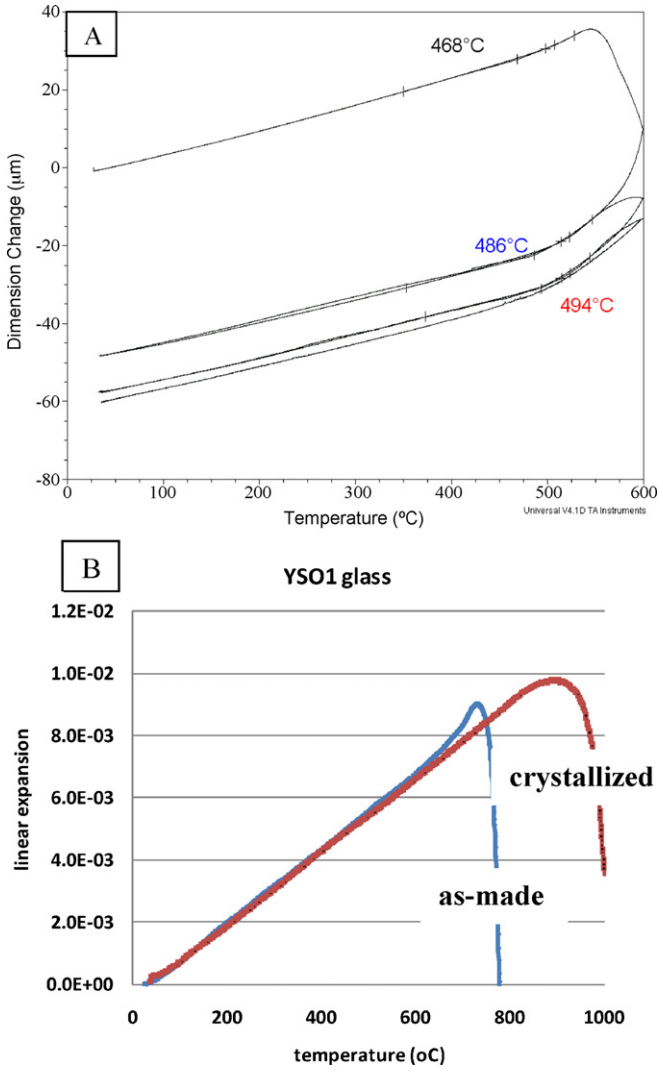

Fig. 3. (A) Typical thermal expansion behavior of glass (SCN-1) during heating and cooling for three times. The number indicates the glass transition point. (B) Typical expansion behavior of a crystallizing glass–ceramics glass sealant (as-made and crystallized).
From Ref. [13].

components (CTE ~ 12.5×10^{-6} °C^{-1}) since the CTE of the NiO–YSZ anode was similar before and after reduction. The fracture of the bilayers in dual environment tests was likely related result of the reduced strength of the bilayer discs after full reduction in reducing gas where more pores (defects) were formed and elasticity was lowered. For example, Radovic and Lara-Curzio found the biaxial strength of sintered NiO/YSZ bilayers decreased from 86 MPa to 68 MPa after reduction at 1000 °C for 30 min where the porosity increased from ~20% to ~37% [23].

3.5. Microstructure and interfacial characterization

The microstructures of the glass matrix and along the glass/YSZ electrolyte and glass/aluminized SS441 interfaces are shown in Figs. 6 and 7, respectively, for the sample aged at 800 °C/1000 h in the dual environment. At the YSZ electrolyte/glass interface, there were localized and concentrated precipitates of "gray" particles whereas in the glass matrix (away from the interface) fewer precipitates were found (Fig. 6). EDS analyses of the selected areas are listed in Table 2. These gray particles are oxides composed mainly of Si (29 at.%), consistent with line scans, with a few percent of Al and K and trace amounts of Na, Mg, Ti, and Zr. The glass matrix shows similar composition but less Si (25.9 at.%) content and some alkaline earths (Ba and Ca). The atomic ratios from these EDS analyses of the gray particle area could not lead to specific silicate compound of these elements (for example simple compound as Na_2SiO_3 and Al_2SiO_5 both are thermodynamically favorable to form at 800 °C with negative Gibbs free energy). Another possibility of common crystalline phase containing K, Al, and Si would be $KAlSi_3O_8$; however, the atomic ratio of K or Al to Si was far from 1:3. This exact nature of these precipitates whether crystalline or amorphous requires further micro-analysis. The current glass contains about 17 wt% of alkalis (K and Na together) and has a low viscosity of 10^5 Pa s (800 °C) (the typical softening point of common glass by its own weight has a viscosity of $10^{6.6}$ Pa s [24]). The low viscosity glass could be more reactive or corrosive since diffusion is much faster in liquids than solids. As a result one would expect to see the dissolution of 8YSZ electrolyte into the glass matrix, and deep migration into the matrix as time progresses if the SCN-1 glass and 8YSZ were not compatible with each other. The fact that EDS area analysis showed no detectible Y and a low concentration of Zr in the glass near the interface seems to indicate the desired chemical compatibility of the compliant SCN-1 glass with YSZ electrolyte.

At the glass and aluminized SS441 interface, no high Si-containing precipitates were found as in the glass/YSZ interface. The alumina coating (point #1 in Fig. 7) remained fairly intact without showing substantial dissolution into the glass matrix, as shown by the elemental line scan where the Al concentration dropped sharply across the alumina coating. Corrosion of alumina or alumina-containing refractory by alkalis to form β-alumina ($NaAl_9O_{14}$) has been of interest for some time due to its use in sodium discharge lamp envelopes [25], in composites [26], structural ceramics, and glass melting [27]. The corrosion can occur either by metal vapor as in the sodium discharge lamp or metal hydroxide as in the combustion-heating furnaces. The corrosion will lead to materials loss by forming β-alumina (for K it has a composition between $K_2O{\cdot}4.75Al_2O_3$ and $K_2O{\cdot}10Al_2O_3$) and structure damage due to large volume expansion (28%) associated with the formation of β-alumina [25]. The current glass contains about 10 wt% K_2O and 7.3% of Na_2O, and was exposed to ambient air and 5%H_2/N_2 with a few percent of moisture (<3%) at 750 and 800 °C for ~1000 h. No β-alumina was identified along the glass/metal interface, which suggests the desirable compatibility between the glass and the alumina coating on the SS441 metal substrate. The long-term stability remains to be evaluated. Nonetheless, the alumina coating was able to minimize Cr diffusion into the glass despite the fact that is was not fully dense and had variations of coverage and thickness. There were some tiny "white" Fe-containing particles next to the alumina coating. The glass matrix (point #2) showed two types of precipitates, equiaxed light particles and darker rod-like precipitates (points #3 and #4, respectively). The chemical compositions of these spots are listed in Table 3. The light particle

Table 2
Chemical analysis of the selected areas in Fig. 5 for sample after 800 °C/1000 h ageing in dual environment. The numbers are in at.%.

Element	#1	#2
O K	66.2	62.9
Na K	0.6	3.2
Mg K	0.2	0.7
A1 K	1.7	1.5
Si K	29	25.9
K K	1.8	3.4
Ca K		1.2
Ba K		1.2
Ti K	0.1	
Zr K	0.3	

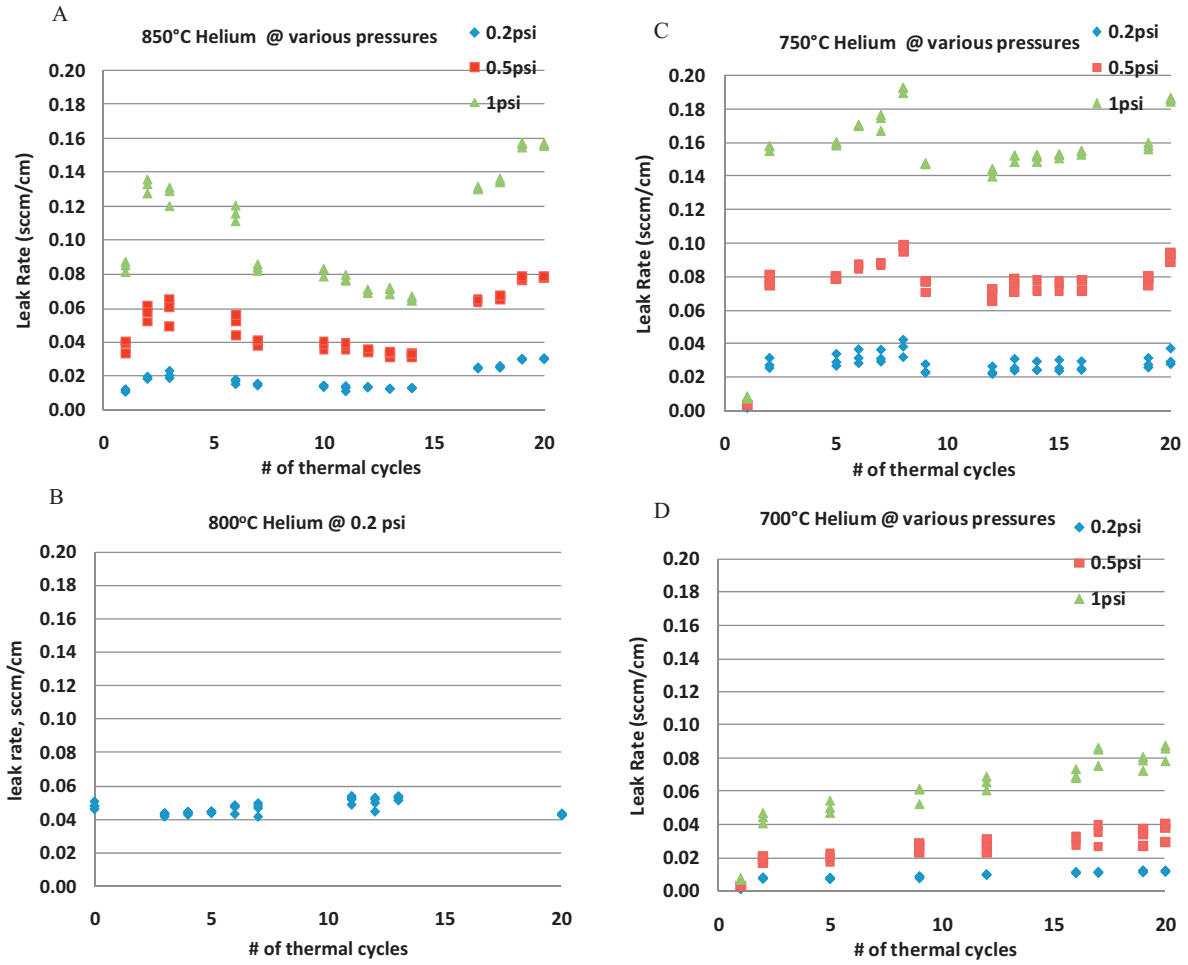

Fig. 4. Thermal cycle stability of SCN-1 glass sealed between ceramic bilayers and aluminized SS441 substrate, and contained between two concentric YSZ rings. The sample was thermally cycled from room temperature to elevated temperatures of: (A) 850 °C, (B), 800 °C, (C) 750 °C, and (D) 700 °C at various helium pressures.

contains primarily Si, Na, and Ca while the dark rod-like precipitates are mostly of Si, Al, and K. The corresponding crystalline phases remain to be determined.

3.6. Self healing and stress considerations for compliant sealing glass

For planar SOFC stacks, the sealing joints are the most critical parts during routine operation with high thermal loads, due to fabrication processes and the service conditions. For sealing glass, whether it is a rigid-type glass–ceramic or a compliant-type non-crystallizing glass, the stress states at operation temperatures are considered minimal. For compliant (non-crystallizing) sealing glasses, any residual stresses can easily be relieved due to the low viscosity since the thermal and elastic properties remain similar to the as-prepared bulk glass. Even for the crystallizing sealing glasses such as Ba–Ca–Al–B-Si (G18) or the more readily crystallized Sr–Ca–Y–B-Si glass (YSO1 in Fig. 3), the volume fraction of crystallites can never approach 100%. There are always some residual glassy phases present at the grain boundaries after formation of the crystallizable phases. As a result, the crystallized glass–ceramics still possess the typical softening behavior and can relieve the stresses at elevated temperatures (although it will take longer as compared to the compliant glasses). Structural damage is most likely to begin during cooling when the glass or glassy phases transform into rigid elastic bodies below the glass transition point; residual stresses (due to mismatch in CTE and elasticity) will continue to build up as the temperature decreases. One may estimate the magnitude of the residual stresses (σ) considering the rigid glass–ceramics (YSO1 glass in Fig. 2B) and the compliant glass (SCN-1 glass in Fig. 2A) with the simple equation:

$$\sigma = E\,\Delta\alpha\,\Delta T$$

where E is the elasticity of the glass, $\Delta\alpha$ is the mismatch of CTE, and ΔT is the temperature difference between the glass transition temperature and room temperature. Using elasticity of 70 GPa for YSO1 glass and 50 GPa for SCN-1, $\Delta\alpha = 0.5 \times 10^{-6}\,^{\circ}C^{-1}$ for YSO1 and $\Delta\alpha = 0.8 \times 10^{-6}\,^{\circ}C^{-1}$ for SCN-1, and $\Delta T = 775\,^{\circ}C$ for YSO1 glass, and $\Delta T = 443\,^{\circ}C$ for SCN-1 glass ($T_g = 468 - 25\,^{\circ}C$), the calculated resid-

Table 3
Chemical analysis of the selected spots in Fig. 6 for sample after 800 °C/1000 h ageing in dual environment. The numbers are in at.%.

Element	#1	#2	#3	#4
O K	58.4	63.0	61.9	63.9
Na K		3.0	6.0	0.9
Mg K		0.9		0.4
A1 K	39.4	1.3	0.3	5.5
Si K	0.2	25.9	22.2	23.4
K K	5.7	3.2	0.9	5.7
Ca K		1.4	7.6	
Ba K		1.4	1.2	0.3
Ti K	0.4			
Cr K	1.0			
Fe K	0.5			

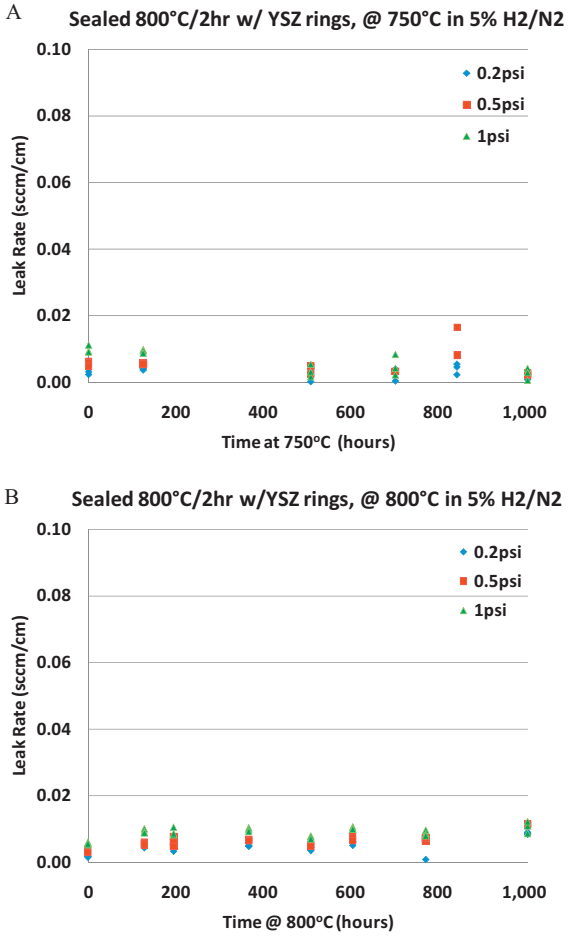

Fig. 5. Isothermal ageing of SCN-1 glass sealed between ceramic bilayers and aluminized SS441 substrate, and contained between two concentric YSZ rings. The samples were tested in dual environment and at elevated temperature of (A) 750 °C and (B) 800 °C.

ual tensile stress was 27 MPa for rigid YSO1 glass–ceramics and ~18 MPa for compliant SCN-1 glass. The stress is indeed smaller for the compliant glass than the rigid glass–ceramics (though it was somewhat overestimated for YSO1 glass since no clear glass transition point can be identified). As brittle fracture is dominated not only by stress but also depends on the flaw size, location, and orientation, the compliant type sealing glass would likely offer flaws with less stress concentration, due to smoother outer surfaces and the lack of crystalline particles. In addition, should cracks initiate and propagate during the cooling cycle, the re-heating to elevated temperatures may well promote the crack healing by capillary actions.

4. Summary and conclusions

A novel alkali-containing compliant silicate sealing glass for SOFC applications was evaluated in terms of thermal cycle stability and chemical compatibility. The glass was sealed between a NiO/YSZ supported YSZ electrolyte disc and an aluminized SS441 substrate, and contained between two YSZ rings. High temperature leak rates were measured between 700 and 850 °C at a differential pressure of 0.2–1.0 psi. All samples showed good thermal cycle stability with hermetic seal behavior in air for 20 deep thermal cycles. The isothermal ageing in dual environment also showed hermetic behavior during the 1000 h isothermal ageing; however, the reduced bilayers fractured after a few thermal cycles. On interfacial microstructure analyses, the alkali-containing glass was found to be compatible with YSZ electrolyte as well as the alumina coating in

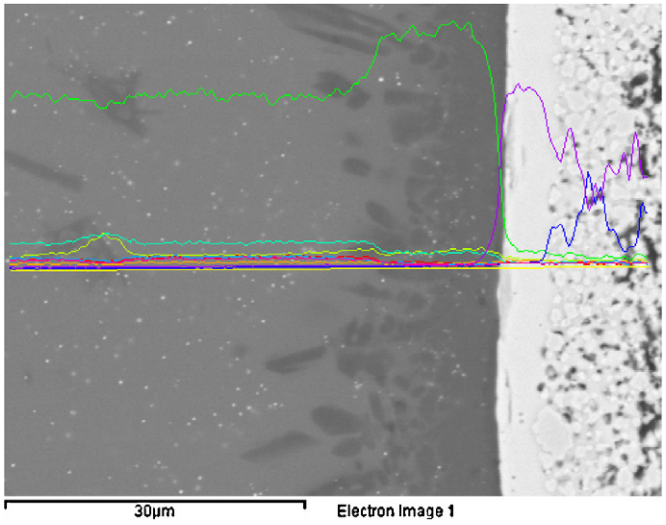

Fig. 6. EDS line scanning along the SCN-1 glass/YSZ electrolyte interface for sample tested at 800 °C/1000 h followed by 4 thermal cycles in dual environment. The elemental analyses in selected rectangular area (1 and 2) are listed in Table 2.

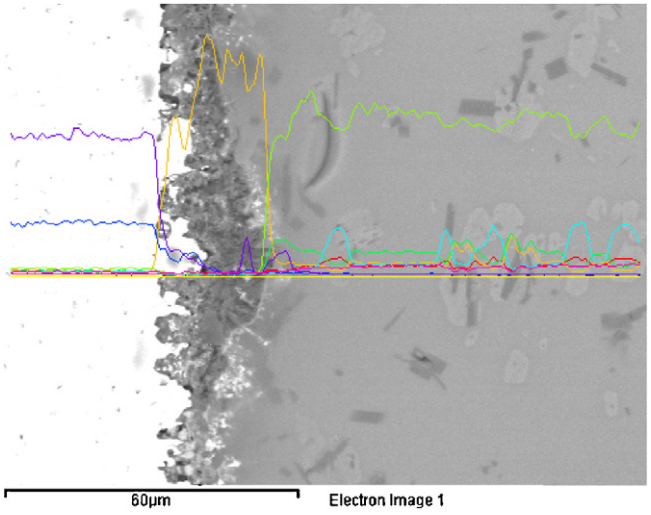

Fig. 7. EDS line scanning along the SCN-1 glass/aluminized SS441 interface for sample tested at 800 °C/1000 h followed by 4 thermal cycles in dual environment. The elemental analyses in selected spots (1, dark alumina coating; 2, glass matrix; 3, white particle; 4, dark particle) are listed in Table 3.

that no discernable reaction or dissolution was found. Simple stress calculations indicated lower stress development during cool down for the compliant sealing glass compared to a devitrifying glass seal. Overall the current study demonstrated the potential applicability of a compliant sealing glass for SOFC sealing applications.

Acknowledgements

The authors would like to thank S. Carlson and J. Coleman (PNNL) and Rosa Trejo (ORNL) for SEM sample preparation and analysis. This paper was funded through the Solid-State Energy Conversion Alliance (SECA) Core Technology Program by the US Department of Energy's National Energy Technology Laboratory (NETL). Pacific Northwest National Laboratory is operated by Battelle Memorial Institute for the US Department of Energy under Contract no. DE-AC06-76RLO 1830. Oak Ridge National Laboratory is operated by UT-Battelle, LLC for the US Department of Energy under Contract no. DE-AC05000OR227250.

References

[1] N.Q. Minh, J. Am. Ceram. Soc. 76 (3) (1993) 563–588.
[2] S.S. Tam, Presented at the 11th Annual SECA Workshop, Pittsburgh, PA, July 27–29, 2010.
[3] Y.S. Chou, J.W. Stevenson, J. Mater. Eng. Perform. 15 (4) (2006) 414–421.
[4] X. Qi, F.T. Akin, Y.S. Lin, J. Membr. Sci. 193 (2) (2001) 185–193.
[5] S. Taniguchi, M. Kadowaki, T. Yasuo, Y. Akiyama, Y. Miyake, K. Nishio, J. Power Sources 90 (1) (2000) 163–169.
[6] K.L. Ley, M. Krumpelt, R. Kumar, J.h. Meiser, I. Bloom, J. Mater. Res. 11 (6) (1996) 1489–1493.
[7] V.A.C. Haanappel, V. Shemet, I.C. Vinke, S.M. Gross, T.H. Koppitz, N.H. Menzler, M. Zahid, W.J. Quadakkers, J. Mater. Sci. 40 (7) (2005) 1583–1592.
[8] N. Lahl, D. Bahadur, K. Singh, L. Singheiser, K. Hilpert, J. Electrochem. Soc. 149 (5) (2002) A607–614.
[9] N. Lahl, K. Singh, L. Singheiser, K. Hilpert, D. Bahadur, J. Mater. Sci. 35 (12) (2000) 3089–3096.
[10] S.-B. Sohn, S.-Y. Choi, G.-H. Kim, H.-S. Song, G.-D. Kim, J. Non-Cryst. Solids 297 (2–3) (2002) 103–112.
[11] P.H. Larsen, P.F. James, J. Mater. Sci. 33 (10) (1998) 2499–2507.
[12] K.D. Meinhardt, D.-S. Kim, Y.-S. Chou, K.S. Weil, J. Power Sources 182 (1) (2008) 188–196.
[13] Y-S. Chou, J.W. Stevenson, P. Singh, J. Electrochem. Soc. 154 (7) (2007) B644–B651.
[14] Y.-S. Chou, J.W. Stevenson, K.D. Meinhardt, J. Am. Ceram. Soc. 93 (3) (2010) 618–623.
[15] Y.-S. Chou, J.W. Stevenson, G.-G. Xia, Z.-G. Yang, J. Power Sources 195 (17) (2010) 5666–5673.
[16] Y.-S. Chou, J.W. Stevenson, J.-P. Choi, J. Electrochem. Soc. 157 (3) (2010) B348–B353.
[17] R.N. Singh, Int. J. Appl. Ceram. Technol. 4 (2) (2007) 134–144.
[18] B.A. Wilson, E.D. Case, J. Mater. Sci. 32 (3) (1997) 3163–3175.
[19] Z. Yang, J.W. Stevenson, K.D. Meinhardt, Solid State Ionics 160 (1) (2003) 213–225.
[20] J.-P. Choi, K. Scott Weil, Y.-S. Chou, J.W. Stevenson, Z.-G. Yang, Int. J. Hydrogen Energy, 2010, in press, doi:10.1016/j.ijhydene.2010.04.110.
[21] Y.-S. Chou, J.W. Stevenson, J. Power Sources 140 (2) (2005) 340–345.
[22] Y.-S. Chou, J.W. Stevenson, J. Power Sources 157 (2) (2006) 260–270.
[23] M. Radovic, E. Lara-Curzio, Acta Mater. 52 (20) (2004) 5747–5756.
[24] W. Vogel, Chemistry of Glass, American Ceramic Society, Inc., OH, 1985, p. 23.
[25] J.A.M. van Hoek, F.J.J. van Loo, R. Metselaar, J. Am. Ceram. Soc. 75 (1) (1992) 109–111.
[26] S.K. Sundaram, J.-Y. Hsu, R.F. Speyer, J. Am. Ceram. Soc. 77 (6) (1994) 1613–1623.
[27] K.E. Spear, M.D. Allendorf, J. Electrochem. Soc. 149 (12) (2002) B551–B559.